Proceedings of the 13th European Workshop on Advanced Control and Diagnosis - ACD2016
Graduate School of Engineering “Hautes Etudes d'Ingenieur”, Lille, France
17 - 18 November 2016

Benchmarking of Advanced Control Strategies for a Simulated Hydroelectric System

S. Finotti, S. Simani, S. Alvisi, M. Venturini

Dipartimento di Ingegneria, Università degli Studi di Ferrara. Via Saragat 1E – 44122 Ferrara (FE), Italy

E-mail: simona.finotti@student.unife.it,
{silvio.simani,stefano.alvisi,mauro.venturini}@unife.it

Abstract. This paper analyses and develops the design of advanced control strategies for a typical hydroelectric plant during unsteady conditions, performed in the Matlab and Simulink environments. The hydraulic system consists of a high water head and a long penstock with upstream and downstream surge tanks, and is equipped with a Francis turbine. The nonlinear characteristics of hydraulic turbine and the inelastic water hammer effects were considered to calculate and simulate the hydraulic transients. With reference to the control solutions addressed in this work, the proposed methodologies rely on data–driven and model–based approaches applied to the system under monitoring. Extensive simulations and comparisons serve to determine the best solution for the development of the most effective, robust and reliable control tool when applied to the considered hydraulic system.

1. Introduction

Hydroelectric plants convert hydraulic energy into useful energy (mainly electric and mechanical energy). Hydropower is, in fact, the most widely adopted form of renewable energy in the world today, accounting for approximately 16% of global energy production, *i.e.* 3673.1 TWh of energy are consumed from hydropower in various countries [1]. With increasing demand for electricity, and concern about reducing fossil fuel consumption, hydropower is likely to continue to play a key role in global energy production. Indeed, changing conditions in the power market have led to an increase in the demand of peak energy generation, short response time and fast frequency changes. Hydroelectric power plants thus need to be operated accounting for different load conditions. More in general, in the operation of hydropower systems the occurrence of variations in the flow is frequently experienced, being true both in routine operation and in accidental or exceptional unforeseen events. The turbine operations such as start–up, load acceptance, load rejection and shutdown may result in hydraulic transients, which can cause large pressure and sub–pressure oscillations in turbine hydraulic systems and must be evaluated to avoid mechanical failures. Matlab and Simulink represent interactive tools for modelling, simulating, and analysing dynamic systems that have been successfully applied also for nonlinear dynamics investigations in hydroelectric processes [2]. Furthermore, power plants are usually equipped with particular control systems to ensure stable operation. The design of proper control systems for hydraulic turbines remains a challenging and important problem.

This paper considers the simulation and the development of different control solutions for a typical hydroelectric power plant, which has a high water head and a long penstock

with upstream and downstream surge tanks, and is equipped with a Francis turbine [3]. In the proposed control systems, an electric servomotor is used as a governor. The nonlinear characteristics of hydraulic turbine and the inelastic water hammer effect were considered to calculate and simulate hydraulic transients. The hydraulic system is described by a nonlinear model, therefore, most of compensation schemes use conventional controllers like on–off strategies, including standard PID regulators for their relative simplicity. However, these controllers do not always produce fast response and suffer the problem of high overshoot and large settling time. Moreover, the tuning of the conventional controllers can be difficult [2]. To this aim, Artificial Intelligence (AI) has been applied to control designs due to substantial advantages of applicability to nonlinear systems with unknown or partially known dynamics [4].

In the last years, AI based methods, namely, Fuzzy Logic (FL), Adaptive Neuro–Fuzzy Inference System (ANFIS), Artificial Neural Network (ANN) and Model Predictive Controllers (MPC) have been considered [5, 6, 4]. When used for fault diagnosis and fault tolerant control purpose, some of these controllers have advantages compared to conventional ones, as shown by the same authors *e.g.* in [7, 8, 9].

Regarding classic compensation strategies applied to hydroelectric systems, several methodologies have been proposed in the literature [10]. They can use optimal control theory [11] or intelligent approaches [12].

The contribution of the paper consists of analysing different control designs already considered by the same authors in [8, 9] but for fault diagnosis and fault tolerant control with application to the simulated hydraulic system described in [7]. Moreover, the simulations and the comparisons with the achieved performances that have been implemented in the Matlab and Simulink environments serve to define the most viable and practical control tool when applied to the considered hydroelectric model. On the other hand, the proposed design tools are fundamental for the assessment, the verification and the validation of the considered control strategies in connection with the most important features of the hydroelectric system.

The paper is organised as follows. The mathematical model of the hydroelectric system is summarised in Section 2. Section 3 analyses the proposed control methods. The achieved results are summarised in Section 4. Comparisons among the different control methods and their performances with respect to measurements and modelling errors are also investigated and discussed. Finally, Section 6 concludes the paper by summarising the main achievements of the work, and providing some suggestions for further research topics.

2. Hydroelectric System

The hydroelectric power plant considered in this work is described in detail in [7]. It consists of a reservoir with water constant level, an upstream water tunnel, an upstream surge tank, a penstock, a downstream surge tank, and a downstream tail water tunnel. Finally, a tail water lake has water constant level.

The expressions (1) and (2) represent the non–dimensional flow rate and water pressure in terms of the corresponding relative deviations:

$$\frac{Q}{Q_r} = 1 + q \tag{1}$$

$$\frac{H}{H_r} = 1 + h \tag{2}$$

where q is the flow rate relative deviation, h the water pressure relative deviation, Q_r and H_r the rated flow rate and the rated water pressure, respectively. With reference to a pressure water supply system, the Newton's second law for a fluid element inside a tube and the conservation mass law for a control volume, which accounts for water compressibility and tube elasticity, can be written. Under the assumption that the penstock is short or medium in length, water and

pipeline can be considered incompressible and rigid, respectively. Therefore, (3) considers only the inelastic water hammer effect:

$$\frac{h}{q} = -T_w\, s - H_f \tag{3}$$

where s is the derivative operator. Under this assumption, the expression (3) represents the flow rate deviation and the water pressure deviation transfer functions for a simple penstock, where H_f is the hydraulic loss and T_w is the water inertia time:

$$T_w = \frac{L\, Q_r}{g\, A\, H_r} \tag{4}$$

depending on the penstock length L, the rated flow rate Q_r, the gravity acceleration g, the cross–section area A, and the rated water pressure H_r.

Regarding the Francis turbine described in [7], the second order polynomial curve (5) relates the non–dimensional water flow rate Q/Q_r to the non–dimensional rotational speed n/n_r. The non–dimensional parameter G (varying in the range between 0 and 100%) represents the turbine wicked gate opening.

$$\frac{Q}{Q_r} = G\left[a_1\left(\frac{n}{n_r}\right)^2 + b_1\left(\frac{n}{n_r}\right) + c_1\right] = f_1\left(n, G\right) \tag{5}$$

The non–dimensional turbine torque M in (6) is a function of the water flow rate Q, the water pressure H, and the rotational speed n. According to the relation (5), the turbine torque M is a function of the water flow rate Q, the rotational speed n and wicked gate opening G.

$$\frac{M}{M_r} = \frac{\frac{Q}{Q_r}\frac{H}{H_r}}{\frac{n}{n_r}} = f_2\left(Q, n, G\right) \tag{6}$$

Finally, the relations (7) and (8) express all the non–dimensional parameters for the turbine in terms of the corresponding relative deviations.

$$\frac{n}{n_r} = 1 + x \tag{7}$$

$$G = 1 + y \tag{8}$$

where q_t represents the turbine flow rate relative deviation, h_t the turbine water pressure relative deviation, x the turbine speed relative deviation, and y the wicket gate servomotor stroke relative deviation. Note that, since G varies in the range $0\% - -100\%$, the definition of (8) makes y vary in the range between -1 and 0.

If the generator unit supplies an isolated load, then the dynamic process of the generator unit considering the load characteristic is represented as [7]:

$$\frac{x}{m_t - m_{g0}} = \frac{1}{T_a\, s + e_g} \tag{9}$$

where m_{g0} is the load torque, T_a the generator unit mechanical time, and e_g the load self–regulation factor. The relationship between the control signal u and the wicket gate servomotor stroke y is thus expressed by means of a first–order model:

$$\frac{y}{u} = \frac{1}{T_y\, s + 1} \tag{10}$$

where T_y is the wicket gate servomotor response time.

3. Control Scheme Design

The general description of the dynamic model of the hydroelectric system can be represented by the nonlinear dynamic function $\mathcal{F}$:

$$u(t) = \mathcal{F}\left(x(t)\right) \tag{11}$$

where x is the process output, u represents the control input, and t is the time. The control strategy applied to the system should determine the control input $u(t)$ such that the controlled process output $x(t)$ is able to track a given reference or set–point $r(t)$.

It can be shown that a continuous–time linearised state–space description of the hydroelectric system can be described by the model (12):

$$\begin{cases} \dot{x}_s(t) &= A_s\, x_s(t) + B_s\, u(t) \\ x(t) &= C_s\, x_s(t) \end{cases} \tag{12}$$

where $x_s \in \Re^6$ represents the state–space vector for the hydroelectric model described in Section 2. The matrices A_s, B_s and C_s of the state–space model have appropriate dimensions. With reference to the model of Eq. (12), the monitored output $x(t)$ represents the turbine speed relative deviation, whilst the control variable is $u(t)$ that is applied to the servomechanism for actuating the wicket gate servomotor stroke relative deviation y according to Eq. (10).

This paper recalls different control strategies including the standard PID controller as well as AI techniques, such as fuzzy logic, adaptive, model predictive controllers, which are used for the regulation of the hydroelectric system. These methodologies are briefly outlined in the following subsections.

3.1. Standard PID Controller

Standard PID regulators are the most commonly used feedback controllers for industrial processes. The control logic is based on the computation of the error $e(t)$ between the desired and the measured values of the output, *i.e.* $e(t) = r(t) - x(t)$, which is fed back to the system after proportional, integral and derivative operations. In this way, the continuous–time control law of the PID regulator is described by Eq. (13):

$$u(t) = K_p\, e(t) + K_i \int_0^t e(\tau)\, d\tau + K_d \frac{de(t)}{dt} \tag{13}$$

where K_p, K_i, K_d are the PID proportional, integral, and derivative gains. The optimal selection of this gains is performed by using the automatic tuning algorithm in the Simulink environment that balances the performance (response time) and the robustness (stability margins) of the controlled system [13].

The PID automatic tuning Simulink toolbox uses the linearised model (12) of the hydroelectric system.

3.2. Fuzzy Controller

Fuzzy Logic Controllers (FLCs) are extensively used in processes where the system dynamics are either very complex or exhibit highly nonlinear characteristics. The controller design approach relies on the identification of transparent rule–based Takagi–Sugeno (TS) fuzzy models using an Adaptive Neuro–Fuzzy Inference System (ANFIS) tool implemented in the Simulink toolbox. The same authors have already proposed the use of fuzzy regulators for the problem of the fault tolerant control design as shown in [8, 9].

The TS fuzzy model consists of a set of rules R_i, where the consequents are deterministic functions f_i:

$$R_i : IF\, x\, is\, A_i\, THEN\, u_i = f_i(x) \tag{14}$$

with $i = 1, 2, \ldots, K$ and K is the number of clusters or rules of the rule–based system, x represents the input vector of the *antecedent* variables, and u_i describes the *consequent* output. A_i represents the antecedent fuzzy set of the i–th rule, defined by its (multivariable) membership function $\mu_{A_i}(x) \rightarrow [0, 1]$ The function f_i is represented by suitable parametric models, whose structure remains equal in all rules, whilst the parameters can vary. A parametrisation in affine form is usually exploited, and described by Eq. (15):

$$u_i = a_i\, x + b_i \tag{15}$$

where the vector a_i and the scalar b_i are the i–th submodel parameters. The vector x contains a suitable number n of delayed samples of the model inputs and output. In this way, the product $a_i\, x$ represents an Auto–Regressive eXogenous (ARX) parametric dynamic model of order n.

The final output u of the TS fuzzy model is the weighted average of all rule outputs, computed as:

$$u = \frac{\sum_{i=1}^{K} \mu_{A_i}(x)\, y_i(x)}{\sum_{i=1}^{K} \mu_{A_i}(x)} \tag{16}$$

The modelling approach used by ANFIS is similar to many system identification techniques. First, the TS fuzzy model structure described by the its order n, the form of the membership functions μ_{A_i} and the number of clusters K are hypothesised. Next, the input–output data are used by ANFIS for training the TS model according to a chosen error criterion, thus determining the optimal values of the controller parameters a_i and b_i [5].

The paper considers also an alternative approach to ANFIS for the derivation of the controller fuzzy model, which is represented by the Fuzzy Modelling and Identification (FMID) toolbox developed in the Matlab environment [5]. Also in this case, the estimation of the controller prototype relies on the identification of rule–based fuzzy models and using the input–output data acquired from the controlled process. This method exploits Takagi–Sugeno fuzzy models and employs the Gustafson–Kessel clustering method to divide the data into subsets with a common local linear (affine) behaviour [5].

The identified fuzzy controller is thus obtained by selecting an proper model structure n and a number of clusters K. The FMID toolbox provides the parameters a_i, b_i and the estimation of the membership functions μ_{A_i} of the optimal controller minimising the tracking error $e(t)$.

Note finally that the fuzzy controller in the form of Eq. (16) is described by a discrete–time input–output model, which is connected to the controlled continuous–time nonlinear system of Eq. (11) using Digital–to–Analog (D/A) and Analog–to-Digital (A/D) converters.

3.3. Linear Adaptive Controller

The adaptive control method exploited in this paper is based on the on–line identification of a second order discrete–time transfer function of an ARX time–varying model in the form:

$$G(z) = \frac{b_1\, z^{-1} + b_2\, z^{-2}}{1 + a_1\, z^{-1} + a_2\, z^{-2}} \tag{17}$$

whose parameters are recursively estimated at each sampling time $t_k = k\,T$, with $k = 1, 2, \ldots, N$, N the number of samples, and T the sampling interval. z represents the unit advance operator. The parameters in (17) are estimated using the Recursive Least–Square Method (RLSM) with directional forgetting factor [13]. The same authors have proposed similar approaches but for fault tolerant control applications, as shown in [8].

The synthesis of the adaptive control law is derived using a modified Ziegler–Nichols criterion, in the form of Eq. (18):

$$u_k = q_0\, e_k + q_1\, e_{k-1} + q_2\, e_{k-2} + (1 - \gamma)\, u_{k-1} + \gamma\, u_{k-2} \tag{18}$$

where e_k is the tracking error $e(t)$ at the sampling time t_k, u_k the control signal $u(t)$ at the sampling time t_k, whilst q_0, q_1, q_2, and γ are the time–varying controller parameters, which are calculated by solving a Diophantine equation that leads to the following relations [13]:

$$\begin{array}{l} q_0 = \frac{1}{b_1}\,(d_1 + 1 - a_1 - \gamma)\,,\ \gamma = q_2\,\frac{b_2}{a_2} \\ q_1 = \frac{a_2}{b_2} - q_2\,\left(\frac{b_1}{b_2} - \frac{a_1}{a_2} + 1\right),\ q_2 = \frac{s_1}{r_1} \end{array} \tag{19}$$

where $r_1 = (b_1 + b_2)\,(a_1\,b_2\,b_1 - a_2\,b_1^2 - b_2^2)$ and $s_1 = a_2\,((b_1 + b_2)\,(a_1\,b_2 - a_2\,b_1) + b_2\,(b_1\,d_2 - b_2\,d_1 - b_2))$. It is assumed that the final closed loop model has a behaviour similar to a second–order continuous time system with characteristic polynomial $s^2 + 2\,\delta\,\omega\,s + \omega^2$, where δ and ω represent its damping factor and natural frequency, respectively. In this case, if $\delta \leq 1$, $d_1 = -2\,e^{-\delta\,\omega\,T}\,\cos\left(\omega\,T\sqrt{1-\delta^2}\right)$ and $d_2 = e^{-2\,\delta\,\omega\,T}$.

Both the on–line identification procedure and the adaptive controller parameter computation are implemented in the self–tuning controller Simulink library [13]. In this way, the sampled output y_k of the time–varying ARX model (17) should follow the sampled reference signal r_k when regulated by the control law (18).

Note finally that, also in this case, the adaptive controller (18) is connected to the continuous–time nonlinear system (11) using the D/A and A/D converters.

3.4. Model Predictive Control

Model Predictive Control (MPC) relies on dynamic models of the process, most often linear models obtained by system identification or linearisation of a nonlinear plant. The main advantage of MPC is the fact that it allows the current sampling time to be optimised, while keeping future sampling times in account. This is achieved by optimising a finite time–horizon, but only implementing the current sampling time. MPC has the ability to anticipate future events and can take control actions accordingly. PID controllers do not have this predictive ability. MPC is nearly universally implemented as a digital control.

MPC is based on iterative, finite–horizon optimisation of the plant model. At the sample k ($k = 1, 2, \ldots, N$) the current plant output is sampled and a cost minimising control strategy is computed (via a numerical minimisation algorithm) for a relatively short time horizon in the future: $[k, k + N_p]$. Specifically, an online calculation is used to explore state trajectories that emanate from the current state and find (via the solution of Euler–Lagrange equations) a cost–minimising control strategy until time $k + N_p$. Only the first step of the control strategy is implemented, then the plant state is sampled again and the calculations are repeated starting from the new current state, yielding a new control and new predicted state path. The prediction horizon keeps being shifted forward and for this reason MPC is also called receding horizon control. The same authors have recently proposed a similar approach, but for the fault tolerant control problem, as shown in [14].

An example of a cost function J for optimisation is given by:

$$J = \sum_{k}^{k+N_p} w_{x_k}\,(r_k - x_k)^2 + \sum_{k}^{k+N_c} w_{u_k}\,\Delta u_k^2 \tag{20}$$

where w_{x_k} the weighting coefficient reflecting the relative importance of the monitored output x_k, and w_{u_k} the weighting coefficient penalising relative big changes in u_k, with $\Delta u_k = u_k - u_{k-1}$. N_p represents the prediction horizon, whilst N_c the control horizon.

Note finally that the discrete–time MPC design is performed by using the MPC toolbox in the Simulink environment, which computes a linearisation of the hydroelectric nonlinear model (12). The discrete–time MPC is thus connected to the continuous–time nonlinear system of Eq. (11) using the D/A and the A/D converters. The MPC Simulink toolbox uses the linearised model (12) of the hydroelectric system.

4. Results

This study exploits the 4 different control methods described in the previous subsections to regulate the output of the hydroelectric nonlinear system. The simulations are performed in the Simulink environment and the toolboxes described above. The achieved results are compared in terms of settling time T_s, maximum overshoot $S\%$ and the percent Normalised Sum of Squared Errors (NSSE), defined as:

$$NSSE\% = 100 \sqrt{\frac{\sum_{k=1}^{N} (r_k - x_k)^2}{\sum_{k=1}^{N} r_k^2}} \tag{21}$$

where r_k and x_k represent the samples of the continuous–time signals $r(t)$ and $x(t)$, respectively. The simulation model with two surge tanks and a Francis turbine described in Section 2 allows the simulation of the behavoir of a hydroelectric power plant in the presence of large hydraulic transients after full load rejection m_{g0}. Usually, the most severe hydraulic transients will happen after full load rejection. Therefore, all of these simulations are performed on full load rejection operating conditions.

The standard control strategy for hydroelectric systems can use a classic PID regulator, whose complete structure has been recalled in Section 3.1. The optimal proportional and integral gains are determined using the automatic PID tuning procedure and settled to $K_p = 0.6567$, $K_i = 0.4468$, $K_d = 1.6567$. This issue was already addressed by the same authors in [7]. The turbine speed governor plays a very important role in hydraulic transients caused by load changes. As already remarked, the classic PID controller proposed earlier in [2] required an optimal tuning of its gains, and in this way only the dynamic performance of the generator unit can be improved. Moreover, in order to get the best dynamic performance, it is necessary to set different optimal PID gains on different operating conditions for turbine speed governor.

The controller capabilities have been assessed in simulation by considering different load torque m_{g0} values, which represent the turbine start–up and shutdown conditions. In particular, the start–up phase is assumed to last 300 s (due to the large size of the considered Francis turbine), while the shutdown maneuver takes just 30 s, to simulate an unplanned emergency shutdown.

4.1. PID Controller Results

As an example, the results summarised in Fig. 1 show that the PID governor of Eq. (13), whose parameters were optimised according to the PID autotuning Simulink toolbox, is able to keep the relative deviation of the rotational speed null ($r(t) = 0$, *i.e.* the rotational speed constant) in steady–state conditions. Its performances are better than the standard PID regulator designed in [2].

In the following, the suggested PID controller, with automatic tuning, together with the classic PID governor, have been implemented and compared in the Matlab and Simulink environments. Regarding the standard PID governor parameters in Eq. (13), they were selected as $K_p = 1.0$, $K_i = 0.2$, $K_d = 1.0$, as described in [2]. On the other hand, the PID governor with automatic tuning will be used as reference controller and compared to the remaining control strategies proposed in this work.

Fig. 1 shows the turbine speed relative deviations x when the load torque m_{g0} changes in start–up and shutdown conditions. The hydroelectric system output is controlled by the continuous–time PID regulator, as shown in Fig. 1.

Table 1 summarises the achieved results in terms of $NSSE\%$, the per–cent undershoot $s\%$, overshoot $S\%$ and the settling time T_s for different values of the load torque m_{g0}. According to these simulation results, good properties of the proposed autotuning PID controller are highlighted, and they are better than the PID governor [2]. In fact, the autotuning design

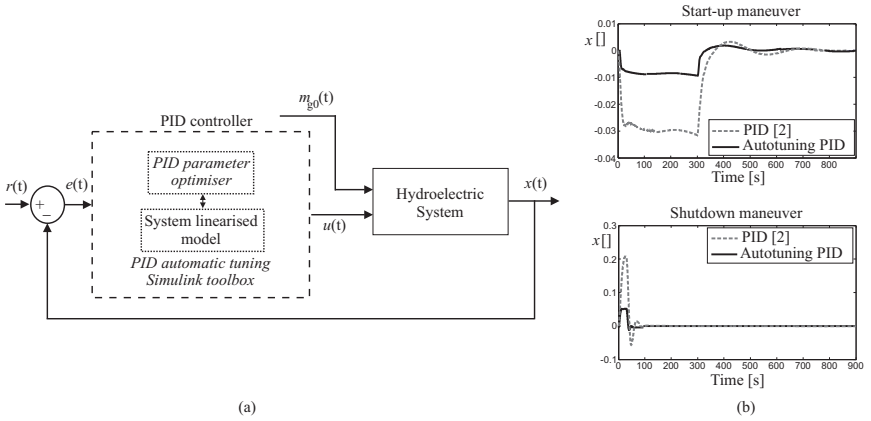

Figure 1. (a) block diagram of the hydroelectric system compensated by the PID regulator with automatic tuning and (b) controlled output.

is able to limit the effect of high–gains for the proportional and the integral contributions of the PID control. Some further comments can be drawn in general regarding the capability of these autotuning solutions. The $NSSE$ values are considerably lower in case of significant transient maneuvers (*i.e.* start–up and shutdown). On the other hand, though always lower, the settling time T_s is not significantly decreased and remains comparable to that obtainable by means of the PID [2]. This is probably due to the inherent dynamics of the simulated hydraulic systems. Similarly, the per–cent $s\%$ and $S\%$ are decreased in all cases by using the autotuning PID controller, and this effect is mainly highlighted when considering the most severe transients (*i.e.* start–up and shutdown).

Note that standard industrial controllers, such the PID recalled in Section 3.1, are quite simple and have the benefit of quite straightforward implementation. However, when applied to the control of hydroelectric systems, the control laws cannot be very efficient. Therefore, the use of more advanced controller solutions can be motivated.

4.2. Fuzzy Controller Results

With reference to the strategies described in Section 3.2, fuzzy identification is used to derive the models of the controllers by exploiting the so–called model reference control approach [15]. For this purpose, the PID regulator of Fig. 1 represents the reference controller for the generation of the data used by the identification strategy proposed described in Section 3.2. In this way, the fuzzy controller parameters are identified such that the performances in terms of tracking error $e(t)$ are optimised.

In particular, with reference to the TS fuzzy controller derived with the ANFIS tool, a sampling interval $T = 0.1s.$ is exploited. Moreover, the fuzzy controller (16) uses a number $K = 3$ of Gaussian membership functions, with a number of delayed inputs and output $n = 1$. The antecedent vector is thus $x = [e_k, e_{k-1}, u_{k-1}]$. The achieved performances of the controller obtained with the ANFIS tool are shown in Fig. 2.

Using the same data from the PID reference regulator, a second fuzzy controller (16) has been estimated using the FMID tool, with a number of clusters $K = 3$, a number of delays $n = 2$, and the antecedent vector $x = [u_{k-1}, u_{k-2}, r_k, r_{k-1}, y_k, y_{k-1},]$. The FMID tool also provides the optimal estimate of the shapes of the membership functions μ_{A_i}. The implementation scheme and the achieved results are represented and compared in Fig. 2.

Fig. 2 highlights that both the fuzzy regulators perform better than the PID controller with autotuning. Also in this case, the settling times T_s, the maximum overshoot $S\%$, and the

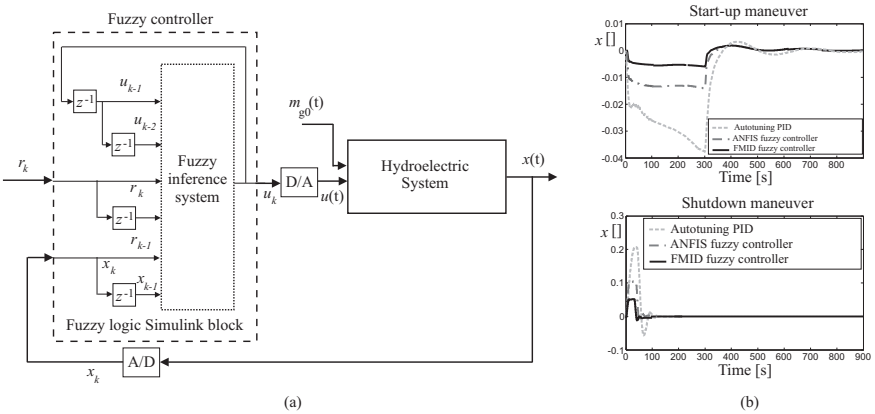

Figure 2. (a) block diagram of the hydroelectric system compensated by the fuzzy regulators and (b) controlled output.

$NSSE\%$ values are reported in Tab. 1, which are computed for the different fuzzy controllers. The simulation results also highlight better properties of the proposed the FMID controller with respect to the ANFIS one, which are motivated by the better capability and flexibility of the FMID tool [5].

4.3. Adaptive Controller Results

On the other hand, by considering the on–line procedure recalled in Section 3.3, Fig. 3 shows the tracking capabilities of the adaptive controller (18). Its time–varying parameters have been obtained via the relations (19) with the damping factor and the natural frequency $\delta = \omega = 1$. The adaptive controller implementation using the Self Tuning controller Simulink Library (STCSL) and the achieved results are reported Fig. 3.

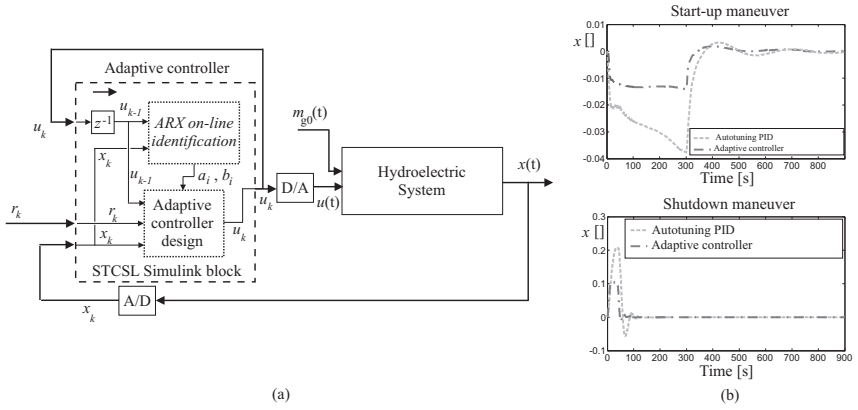

Figure 3. (a) block diagram of the hydroelectric system compensated by the adaptive regulator and (b) controlled output.

Table 1 summarises the achieved results of the adaptive controller in terms of $NSSE\%$, the per–cent undershoot $s\%$, overshoot $S\%$ and the settling time T_s for different values of the load torque m_{g0}. According to these simulation results, good properties of the proposed adaptive controller are highlighted, and they are better than the autotuning PID governor.

4.4. MPC Results

Finally, with reference to the MPC strategy recalled in Section 3.4, the reference and the monitored output signals are depicted in Fig. 4 with its implementation.

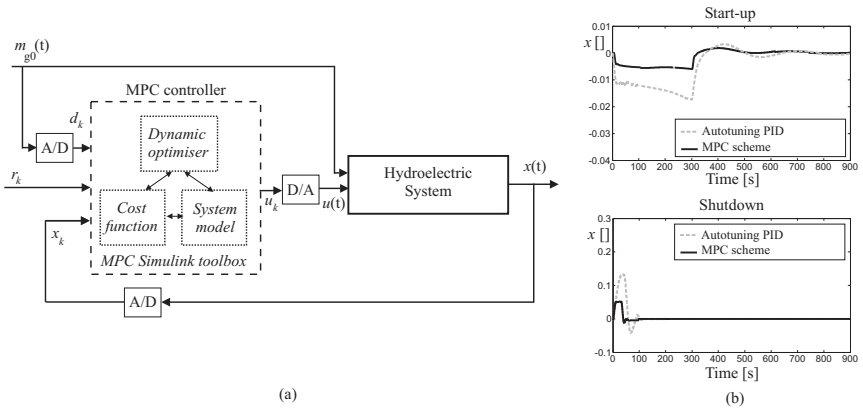

Figure 4. (a) block diagram of the hydroelectric system compensated by the MPC law and (b) controlled output.

The results shown in Fig. 4 have been achieved by using a prediction horizon $N_p = 10$ and a control horizon $N_c = 2$. The weighting parameters have been settled to $w_{y_k} = 0.1$ and $w_{u_k} = 1$, in order to reduce abrupt changes of the control input. Finally, the MPC strategy performance is summarised in Table 1.

4.5. Quantitative Comparison of the Advanced Control Strategies

In order to provide a comparison of the performances obtained by the considered control solutions, Table 1 summarises the achieved results for different values of the load torque.

Table 1. $NSSE\%$, T_s, $s\%$, and $S\%$ for the considered control solutions.

Controller Type	m_{g0}	$NSSE\%$	T_s	$s\%$	$S\%$
PID [2]	+100%	1.86%	725.59s	3.15%	0.32%
	−100%	3.34%	76.05s	5.66%	20.73%
Autotuning PID	+100%	0.62%	701.36s	0.96%	0.12%
	−100%	1.38%	54.08s	1.19%	5.76%
Fuzzy ANFIS	+100%	0.21%	525.59s	3.15%	0.32%
	−100%	0.18%	76.05s	5.66%	20.73%
Fuzzy FMID	+100%	0.17%	501.36s	0.96%	0.12%
	−100%	0.12%	54.08s	1.19%	5.76%
Adaptive controller	+100%	0.32%	601.36s	0.76%	0.09%
	−100%	0.78%	22.08s	0.58%	2.31%
MPC scheme	+100%	0.29%	581.23s	0.64%	0.08%
	−100%	0.67%	19.98s	0.49%	1.99%

Note that the MPC regulator leads to the best values of settling time and maximum overshoot, as its parameters are automatically tuned in the Simulink environment in order to optimise the MPC cost function of Eq. (20), as recalled in Section 3.4.

5. Parameter Sensitivity Analysis

This section analyses the robustness features of the proposed controllers with respect to parameter variations. This analysis exploits the Monte–Carlo tool, as the control performance depends on the model–reality mismatch as well as on the input–output measurement errors. Therefore, the analysis has been performed by describing the hydroelectric model parameters as Gaussian stochastic processes with mean values corresponding to the nominal ones and standard deviations of $\pm 20\%$. The average $NSSE\%$ index values have been computed with 100 Monte–Carlo runs, and summarised in Table 2.

Table 2. Monte–Carlo analysis for the designed controllers: $NSSE\%$ average values with parameter variations.

Controller type	Torque value m_{g0}	Average $NSSE\%$
PID [2]	+100%	5.67%
	−100%	20.67%
Autotuning PID	+100%	1.35%
	−100%	10.59%
Fuzzy ANFIS	+100%	1.22%
	−100%	0.96%
Fuzzy FMID	+100%	1.01%
	−100%	0.41%
Adaptive controller	+100%	1.18%
	−100%	3.96%
MPC scheme	+100%	0.19%
	−100%	0.22%

It is worth noting that, with reference to the values summarised in Table 2 achieved via the Monte–Carlo analysis, they can serve to compare the overall behaviour of the considered controllers in transient conditions with respect to the standard PID solution. Moreover, the values in Table 2 suggest that when the modelling of the dynamic system can be taken into account, the MPC scheme is preferred, even if an optimisation procedure is required. However, in the case of a system with modelling errors, after a certain amount of off–line learning, the fuzzy–based estimation error can fall below the value of the MPC–based scheme, as shown for the controller estimated via the FMID tool. On the other hand, the FMID controller achieves the best control capabilities. The adaptive approach takes advantage of its improved features, as it is able to track possible variations of the controlled system, but with quite complicated and not straightforward design procedures. The fuzzy–based schemes rely on the learning accumulated from off–line simulations, but the training stage can be computationally heavy. Regarding the standard PID control strategy, it is rather simple and straightforward, even if the achievable performances are quite limited. Similar results, but with application to different dynamic processes, were addressed by the same authors in [16, 17].

6. Conclusion

This paper addressed the design of advanced control strategies for a hydroelectric power plant modelled in the Matlab and Simulink environments. The hydraulic system consisted of a high water head and a penstock with upstream and downstream surge tanks and a Francis turbine. The nonlinear characteristics of hydraulic model were considered to simulate the hydraulic transients and to evaluate the behaviour of the proposed hydraulic turbine regulating systems. The suggested control methodologies were designed using data–driven and model–based

approaches applied to the system under monitoring. Extensive simulations showed that the model predictive control scheme has to be preferred when the modelling of the dynamic system can be taken into account. However, in case of modelling errors, artificial intelligence schemes can rely on the learning accumulated from off–line simulations, but the training stage can be computationally heavy. On the other hand, adaptive approaches can track variations of the controlled system, but with complex design procedures. Finally, standard PID control solutions are rather simple and straightforward, but the achievable performances are quite limited.

References

[1] R. R. Singh, T. R. Chelliah, and P. Agarwal, “Power electronics in hydro electric energy systems – A review,” *Renewable and Sustainable Energy Reviews*, vol. 32, pp. 944–959, April 2014.

[2] H. Fang, L. Chen, N. Dlakavu, and Z. Shen, “Basic modeling and simulation tool for analysis of hydraulic transients in hydroelectric power plants,” *IEEE Trans. Energy Convers.*, vol. 23, pp. 424–434, Sept. 2008.

[3] M. Popescu, D. Arsenie, and P. Vlase, *Applied Hydraulic Transients: For Hydropower Plants and Pumping Stations*. Lisse, The Netherlands: CRC Press, Jan. 2003.

[4] J. Korbicz, J. M. Koscielny, Z. Kowalczuk, and W. Cholewa, eds., *Fault Diagnosis: Models, Artificial Intelligence, Applications*. London, UK: Springer–Verlag, 1st ed., February, 12 2004. ISBN: 3540407677.

[5] R. Babuška, *Fuzzy Modeling for Control*. Boston, USA: Kluwer Academic Publishers, 1998.

[6] J. Maciejowski, “Modelling and predictive control: enabling technologies for reconfiguration,” *Annual Reviews in Control*, vol. 23, pp. 13–23, 1999.

[7] S. Simani, S. Alvisi, and M. Venturini, “Study of the Time Response of a Simulated Hydroelectric System,” in *Journal of Physics: Conference Series* (H. Schulte and S. Georg, eds.), vol. 570 of *Conference Series*, pp. 1–13, Bristol, United Kingdom: IOP Publishing Limited, Dec. 2014. ISSN: 1742–6596. DOI: 10.1088/1742-6596/570/5/052003.

[8] S. Simani, S. Alvisi, and M. Venturini, “Data–Driven Design of a Fault Tolerant Fuzzy Controller for a Simulated Hydroelectric System,” in *Proceedings of the 9th IFAC Symposium on Fault Detection, Supervision and Safety for Technical Processes – SAFEPROCESS'15* (IFAC, ed.), vol. 48, (Paris, France), pp. 1090–1095, IFAC, Sept. 2–4 2015. DOI: 10.1016/j.ifacol.2015.09.672. ISBN: 978–3–642–27644–6. ISSN: 1474–6670. Special session invited paper.

[9] S. Simani, S. Alvisi, and M. Venturini, “Fault Tolerant Control of a Simulated Hydroelectric System,” *Control Engineering Practice*, vol. 51, pp. 13–25, June 2016. DOI: http://dx.doi.org/10.1016/j.conengprac.2016.03.010.

[10] J. A. Laghari, H. Mokhlis, A. H. A. Bakar, and H. Mohammad, “A comprehensive overview of new designs in the hydraulic, electrical equipments and controllers of mini hydro power plants making it cost effective technology,” *Renewable and Sustainable Energy Reviews*, vol. 20, pp. 279–293, 2013.

[11] P. Schniter and L. Wozniak, “Efficiency based optimal control of kaplan hydro generators,” *IEEE Trans. Energy Conver.*, vol. 10, pp. 348–353, June 1995.

[12] M. Djukanovic, M. Novicevic, D. J. Dobrijevic, B. Babic, J. Dejan, and Y. H. P. Sobajic, “Neural–net based coordinated stabilizing control for the exciter and governor loops of low head hydropower plants,” *IEEE Trans. Energy Conver.*, vol. 10, pp. 760–767, Dec. 1995.

[13] V. Bobál, J. Böhm, J. Fessl, and J. Machácek, *Digital Self–Tuning Controllers: Algorithms, Implementation and Applications*. Advanced Textbooks in Control and Signal Processing, Springer, 1st ed., 2005.

[14] S. Simani, S. Alvisi, and M. Ventirini in *Proceedings of the* 3^{rd} *International Conference on Control and Fault–Tolerant Systems – SysTol'16* (I. Control Systems Society, ed.), (Barcelona, Spain), pp. 1–6, Research Center for Supervision, Safety and Automatic Control of the Universitat Politècnica de Catalunya in Barcelona, IEEE, 7–9 Sept. 2016. (Accepted). Special session invited paper.

[15] M. Brown and C. Harris, *Neurofuzzy Adaptive Modelling and Control*. Prentice Hall, 1994.

[16] S. Simani, “Overview of Modelling and Advanced Control Strategies for Wind Turbine Systems,” *Energies*, vol. 8, pp. 13395–13418, 25 November 2015. Invited paper of the special issue ”Wind Turbine 2015”. ISSN: 1996-1073. DOI: 10.3390/en81112374.

[17] C. Turhan, S. Simani, I. Zajic, and G. Gokcen Akkurt, “Comparative analysis of thermal unit control methods for sustainable housing applications,” in *Proc. of the 12th REHVA World Congress CLIMA 2016*, vol. 8, (Aalborg, Denmark), pp. 1–10, REHVA – Federation of European Heating, Ventilation and Air Conditioning Associations, REHVA, 22–25 May 2016.